

Two-mode squeezing in polariton four-wave mixing

M. Romanelli,¹ J. Ph. Karr,² C. Leyder,² E. Giacobino,² and A. Bramati²

¹*Institut de Physique de Rennes, UMR CNRS 6251, Université de Rennes 1, Campus de Beaulieu, F-35042 Rennes Cedex, France*

²*Laboratoire Kastler Brossel, Université Pierre et Marie Curie, Ecole Normale Supérieure et CNRS,*

UPMC Case 74, 4 place Jussieu, 75252 Paris Cedex 05, France

(Received 23 July 2010; revised manuscript received 8 September 2010; published 15 October 2010)

We present an analytical model describing polariton four-wave mixing oscillation in semiconductor microcavities. The noise spectra of the intensity difference of the light emitted by the oscillating polariton modes are calculated. It is shown that the two-mode squeezing depends essentially on the ratio of the photonic to the excitonic fraction of the polariton modes. This ratio can be adjusted freely by changing the cavity-exciton detuning. A comparison with available experimental results indicates that a significant intensity difference squeezing can be expected for realistic experimental situations.

DOI: [10.1103/PhysRevB.82.155313](https://doi.org/10.1103/PhysRevB.82.155313)

PACS number(s): 42.50.Lc, 71.36.+c

I. INTRODUCTION

The nonlinearities due to excitonic interactions in strongly coupled semiconductor microcavities are at the origin of a wealth of effects that have been recently uncovered, such as condensation,¹ collective fluid dynamics,^{2,3} and superfluidity.⁴ The great relevance of the coherent nonlinear optical response in polariton systems was first realized about 10 years ago, with the discovery of parametric amplification and oscillation of polaritons (Refs. 5–8). The implications of these experimental and theoretical advances for the generation of squeezed and quantum correlated field states was soon pointed out.^{9–12} Based on the squeezing properties demonstrated in media possessing second- and third-order nonlinearities, one could expect analogous quantum effects, involving composite half-matter half-light bosons, to be observed for polariton parametric oscillators.

The coherent nature of the parametric process was demonstrated by Messin *et al.* using a degenerate Kerr-type configuration.⁶ In the same geometry, Karr showed that the light reflected from a microcavity presented an amount of squeezing of 4%.¹³ That was the first experimental evidence of quantum effects in polariton systems, followed by the demonstration of quantum complementarity in the parametric luminescence from microcavity polaritons.¹⁴

In the so-called “magic angle” geometry (i.e., with the pump beam having in-plane wave vector \mathbf{k}_p , giving birth to a strong signal at $\mathbf{k}_s=0$ and a weak idler at $\mathbf{k}_i=2\mathbf{k}_p$), quantum correlations between the signal and idler polaritons are also expected.¹¹ However, it turns out that the strong imbalance in the photonic content of the signal and idler polariton modes makes it extremely difficult to observe such correlations. This problem was solved using a more symmetrical pump scheme, that makes use of two pump beams having opposite wave vectors \mathbf{k}_p and $-\mathbf{k}_p$ (from now on, we drop “in-plane”). In this case, momentum conservation requires $\mathbf{k}_s+\mathbf{k}_i=0$ while energy conservation imposes $|\mathbf{k}_s|=|\mathbf{k}_i|=|\mathbf{k}_p|$. Indeed, in such a configuration, two bright spots lying approximately on a diameter of the $|\mathbf{k}|=|\mathbf{k}_p|$ circle in k space were observed in the far-field emission pattern from the microcavity, above an oscillation threshold (see Fig. 1). Strong intensity correlations were measured between the light emission from the

two spots,¹⁵ however they remained in the classical domain.

A theoretical treatment of the observed four-wave mixing process was provided by Verger *et al.*, including disorder and multiple scattering effects, using a numerical quantum Monte Carlo method.¹⁶ The issue of quantum effects in microcavities was also tackled using the nonequilibrium Langevin approach by Portolan *et al.*^{17–19} Here we present a less general model based on Heisenberg-Langevin equations which provide a simpler but quite efficient approach, that is in our opinion more transparent to physical interpretation. Our model allows to obtain a simple analytical expression for the intensity noise spectrum of the emitted light, a quantity that can be easily measured. Useful hints for future experiments searching for nonclassical effects can be extracted from the derived expressions. In general, the physical properties of polariton systems depend simultaneously on the wave vector k and on the cavity-exciton detuning δ_0 at $k=0$. Our model reveals that the squeezing dependence on k and δ_0 can be expressed using only one parameter, which we denote as s ,

$$s = \frac{\gamma_a C^2}{\gamma_b X^2}, \quad (1)$$

where γ_a and γ_b are the photonic and homogeneous excitonic linewidth, respectively, and C^2 and $X^2=1-C^2$ are the photonic and excitonic fraction of the polariton mode, re-

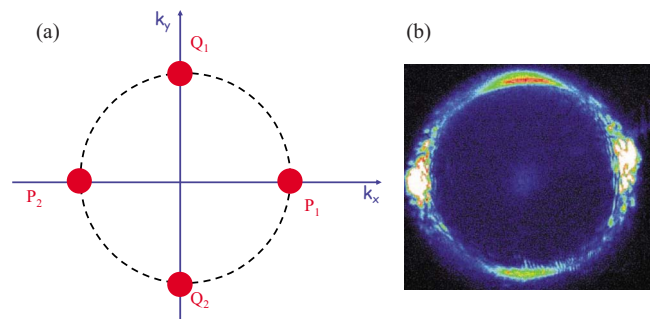


FIG. 1. (Color online) (a) Sketch of the four-wave mixing process under study: the two pump modes P_i and the two generated modes Q_i lie on a circle in k space. (b) Experimental far-field emission pattern (Ref. 15).

spectively. Thus s is the ratio of the photonic to the excitonic fraction, weighted by the respective linewidths. Since C depends on both k and δ_0 , the squeezing dependence on k and δ_0 is automatically accounted for by the single parameter s . In particular, we will discuss the essential role of δ_0 in determining the squeezing performance of the system. Anticipating the results that will be presented in the paper, two main conclusions are the outcome of our analysis: (1) The higher the photonic fraction of the mode, the higher the squeezing that can be obtained. (2) Perhaps more importantly, a high photonic fraction efficiently filters out excess excitonic noise, making the squeezing more robust against it.

From an analysis of previous experimental results, we suggest that a substantial amount of squeezing can be expected for realistic experimental parameters. The following part of the paper is organized as follows. In Sec. II, we derive the Heisenberg-Langevin equations for the polariton modes driven by the external pumps and by fluctuating input fields. Section III is devoted to the study of the stationary state of the system. In Sec. IV, we derive analytical expressions for the fluctuations of the fields. Finally, the results are discussed in Sec. V.

II. HEISENBERG-LANGEVIN EQUATIONS

A. Hamiltonian

We start from the Hamiltonian describing polaritons dynamics in a resonantly excited semiconductor microcavity,⁸

$$\begin{aligned}
 H = & H_{LP} + H_{UP} = \sum_{\mathbf{k}} E_{LP}(k) p_{\mathbf{k}}^\dagger p_{\mathbf{k}} \\
 & + \frac{1}{2} \sum_{\mathbf{k}, \mathbf{k}', \mathbf{h}} V_{\mathbf{k}, \mathbf{k}', \mathbf{h}}^{LP} p_{\mathbf{k}+\mathbf{h}}^\dagger p_{\mathbf{k}'-\mathbf{h}}^\dagger p_{\mathbf{k}} p_{\mathbf{k}'} + \sum_{\mathbf{k}} E_{UP}(k) q_{\mathbf{k}}^\dagger q_{\mathbf{k}} \\
 & + \frac{1}{2} \sum_{\mathbf{k}, \mathbf{k}', \mathbf{h}} V_{\mathbf{k}, \mathbf{k}', \mathbf{h}}^{UP} q_{\mathbf{k}+\mathbf{h}}^\dagger q_{\mathbf{k}'-\mathbf{h}}^\dagger q_{\mathbf{k}} q_{\mathbf{k}'}, \quad (2)
 \end{aligned}$$

where $p_{\mathbf{k}}$ and $q_{\mathbf{k}}$ are the annihilation operators for the polariton mode having wave vector \mathbf{k} , for the lower and upper polariton branch, respectively. In terms of photon and exciton annihilation operators $a_{\mathbf{k}}$ and $b_{\mathbf{k}}$, $p_{\mathbf{k}}$ and $q_{\mathbf{k}}$ read

$$p_{\mathbf{k}} = -C a_{\mathbf{k}} + X b_{\mathbf{k}}, \quad (3)$$

$$q_{\mathbf{k}} = X a_{\mathbf{k}} + C b_{\mathbf{k}}, \quad (4)$$

C and X being the Hopfield coefficients

$$C^2 = \frac{\Omega_R^2}{2\sqrt{\delta_k^2 + \Omega_R^2}(\delta_k + \sqrt{\delta_k^2 + \Omega_R^2})}, \quad (5)$$

$$X^2 = \frac{\delta_k + \sqrt{\delta_k^2 + \Omega_R^2}}{2\sqrt{\delta_k^2 + \Omega_R^2}}. \quad (6)$$

The Hopfield coefficients depend on the Rabi energy Ω_R describing the linear exciton-photon coupling and on the cavity-exciton detuning $\delta_k = E_{cav}(k) - E_{exc}(k)$. The exciton mass being much larger than the photon effective mass, we

can consider that the exciton dispersion is perfectly flat; therefore in the following $E_{exc}(k)$ is regarded as a constant. The photon dispersion reads as

$$E_{cav}(k) = \sqrt{E_0^2 + \hbar^2 k^2 c^2 / n_c^2}, \quad (7)$$

where $E_0 = \hbar c / \lambda_0 = E_{exc} + \delta_0$ is the cavity resonance energy at normal incidence and n_c is the cavity refractive index. Equation (7) can also be written as

$$E_{cav}(i, \delta_0) = \frac{E_{exc} + \delta_0}{\sqrt{1 - \frac{\sin^2 i}{n_c^2}}}, \quad (8)$$

i being the angle of propagation with respect to normal incidence for a photon escaping the cavity, or equivalently for a pump beam driving the polariton mode with wave vector $k = k_0 \sin i / \sqrt{n_c^2 - \sin^2 i}$. From Eq. (8) we see that E_{cav} or equivalently δ_k can be controlled by changing either the incidence angle i or δ_0 . We recall here that microcavity samples are usually wedged, and experimentally a simple translation of the sample allows to change the optical cavity length, i.e., δ_0 .

The polariton energies are given by

$$E_{LP}(k) = \frac{1}{2}(E_{cav}(k) + E_{exc}(k) - \sqrt{\delta_k^2 + \Omega_R^2}), \quad (9)$$

$$E_{UP}(k) = \frac{1}{2}(E_{cav}(k) + E_{exc}(k) + \sqrt{\delta_k^2 + \Omega_R^2}). \quad (10)$$

The energies of the two polariton branches and the Hopfield coefficients are plotted in Fig. 2 as a function of δ_0 . The values of the constants used in all the plots, unless specified, are reported in Table I and correspond to the sample used in Ref. 15.

Nonlinearities are described by the interaction potential $V_{\mathbf{k}, \mathbf{k}', \mathbf{h}}$, which for the lower branch reads

$$V_{\mathbf{k}, \mathbf{k}', \mathbf{h}}^{LP} = [V_0 X_{|\mathbf{k}+\mathbf{h}|} X_{\mathbf{k}'} + 2V_{sat}(C_{|\mathbf{k}+\mathbf{h}|} X_{\mathbf{k}'} + X_{|\mathbf{k}+\mathbf{h}|} C_{\mathbf{k}'})] X_{|\mathbf{k}'-\mathbf{h}|} X_{\mathbf{k}}, \quad (11)$$

where V_0 and V_{sat} are defined as in Ref. 8.

At this point we notice two important facts. First, in Hamiltonian (2) nonlinear couplings between the two polariton branches have been neglected due to the large energy separation between them (typically ~ 5 meV for the III-V samples that we consider²⁰), so that the dynamical evolution of upper and lower polaritons are independent. Second, equations for upper polaritons and lower polaritons are obtained from each other by the correspondences

$$X \mapsto C, \quad (12)$$

$$C \mapsto -X. \quad (13)$$

Therefore, in the following we will only derive the equations for the lower polariton branch. The final results can be generalized to the upper branch with the substitutions (12) and (13).

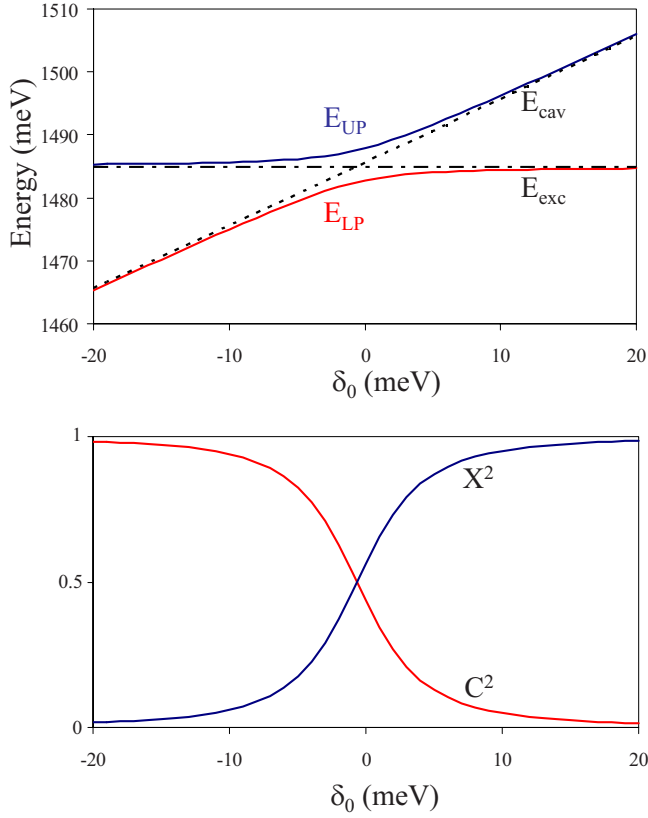


FIG. 2. (Color online) (a) Lower and upper polariton energy branches (solid lines), and cavity and exciton dispersions (dotted lines) as a function of the cavity-exciton detuning δ_0 . (b) Hopfield coefficients.

B. Derivation of the equations of motion

We will model the process sketched in Fig. 1 and experimentally observed in Ref. 15 by considering that only four modes are involved: the two pump modes p_1 and p_2 and the two modes p_3 and p_4 generated by the parametric process. We focus on the regime of four-wave mixing oscillation, in which two strongly correlated polariton populations were observed above the oscillation threshold. In order to neglect multiple scatterings, we assume that the system is slightly above threshold. In this approach, the influence of fluctuations of other modes below threshold is neglected, which is a valid approximation if the signal and idler modes can be effectively separated from the others. An imperfect spatial selection will lead to a reduction in the detected squeezing.

TABLE I. Numerical values of the constants appearing in the formulas.

E_{exc}	1485 meV
i	6°
n_c	3.54
γ_a	0.12 meV
γ_b	0.075 meV
Ω_R	5.07 meV
$\frac{V_{sat}}{V_0}$	0.02

We consider pumping under linear TM polarization and neglect spin dynamics,²¹ therefore implicitly assuming that a perfect polarization inversion takes place, on time scales that are much faster than those involved here. An almost perfectly cross-polarized four-wave mixing emission has been observed,²² therefore the correction is on the order of a few percent at worst. The assumption on adiabatic elimination of polarization dynamics is excellently verified because we are interested in noise spectra at typically megahertz frequencies.

In order to derive the dynamic equations for the system, we only take into account the resonant terms in Eq. (2) that contain the four considered modes. The equation of motion for the operator p_1 in the Heisenberg representation is

$$i\hbar \frac{d}{dt} p_1 = [p_1, H] = [E_{LP}(1) + V(\hat{N}_{p_1} + 2\hat{N}_{p_2} + 2\hat{N}_{p_3} + 2\hat{N}_{p_4})] \hat{p}_1 + 2V\hat{p}_2^\dagger \hat{p}_4 \hat{p}_3, \quad (14)$$

where we have introduced the population operators $\hat{N}_{p_i} = \hat{p}_i^\dagger \hat{p}_i$, and set $V_{\mathbf{k},\mathbf{k}',\mathbf{h}}^{LP} \equiv V = (V_0 X^2 + 4V_{sat} CX) X^2$. We see that there are two types of nonlinearities: energy renormalization due to Kerr-type terms involving the population of each mode, and four-wave mixing described by the term $2V\hat{p}_2^\dagger \hat{p}_4 \hat{p}_3$. The equation for p_2 can be obtained by exchanging p_1 and p_2 in Eq. (14) while the equations for p_3 and p_4 are obtained by the exchanging p_1 with p_3 and p_2 with p_4 . We note that the interaction potential V has the same value everywhere because the modulus of the wave vector is the same for all the modes involved [Eq. (11)].

1. Dissipation and input fluctuations

Equation (14) describes an unitary evolution. In order to take into account polariton relaxation, we adopt a phenomenological treatment by including the following terms in the evolution equation [Eq. (14)]:

$$- \gamma \hat{p}_1 + \hat{p}_1^{in}(t), \quad (15)$$

where γ is the polariton linewidth

$$\gamma = C^2 \gamma_a + X^2 \gamma_b \quad (16)$$

written as a linear combination of the cavity mode linewidth γ_a and of the homogeneous exciton linewidth γ_b . The first contribution in Eq. (15) represents dissipation due to mirror transmission and exciton relaxation. The second contribution describes input fluctuations for the polariton mode, due to the dissipative couplings with two reservoirs, the vacuum modes of the electromagnetic field and the exciton reservoir, respectively.

Following Karr *et al.*,¹¹ we write the input fluctuations operator $\hat{p}_1^{in}(t)$ as a linear combination of the photonic and excitonic fluctuations operators,

$$\hat{p}_1^{in}(t) = -C\sqrt{2\gamma_a} \hat{A}_1^{in} + X\sqrt{2\gamma_b} \hat{B}_1^{in}, \quad (17)$$

where γ_a (γ_b) and \hat{A}_1^{in} (\hat{B}_1^{in}) are the relaxation rate for the photons (excitons) and the input photonic (excitonic) field, respectively.

One important approximation made in the present approach is to treat separately the photon and exciton relax-

ation. That is, we neglected modifications induced by the strong coupling between exciton and photons, which originate from the peculiar shape of the polariton dispersion relation. It is necessary to stress that an *ab initio* treatment of the polariton relaxation and of the associated input fluctuations is extremely complex. In order to derive the statistical properties of the operator \hat{P}_1^{in} , one should take into account elastic and inelastic scattering processes, as well as the interaction with acoustic phonons. These issues have been considered early by Tassone,²³ and more recently by Portolan.¹⁸ Here we will not try to address the issue of the calculation of the polariton input noise. Instead, we will deduce the amount of the input excitonic noise in a given polariton mode directly from the experimental data, i.e., from the experimentally measured intensity noise of the light emitted from the microcavity, under the assumption (experimentally verified) that the input photonic field is in a coherent state. Some more considerations on input fluctuations are developed in Sec. V.

2. Slowly varying operators

We eliminate fast oscillations at the optical frequency by introducing the slowly varying operators $\hat{p}_i = \hat{p}_i e^{i\omega_L t}$, where ω_L is the pump laser frequency.

We then introduce the following normalized quantities and operators:

$$\hat{P}_i = \sqrt{\frac{g}{\gamma}} \hat{p}_i \quad (i=1,2), \quad (18)$$

$$\hat{Q}_i = \sqrt{\frac{g}{\gamma}} \hat{q}_i \quad (i=3,4), \quad (19)$$

$$g = \frac{2V}{\hbar}, \quad (20)$$

$$\Delta_i = \frac{\delta_i}{\gamma} = \frac{\omega(i) - \omega_L}{\gamma}, \quad (21)$$

$$\hat{P}_i^{in} = -C \sqrt{\frac{2\gamma_a g}{\gamma^2}} \frac{\hat{A}_i^{in}}{\sqrt{\gamma}} + X \sqrt{\frac{2\gamma_b g}{\gamma^2}} \frac{\hat{B}_i^{in}}{\sqrt{\gamma}} \quad (i=1,2), \quad (22)$$

$$\hat{Q}_i^{in} = -C \sqrt{\frac{2\gamma_a g}{\gamma^2}} \frac{\hat{A}_i^{in}}{\sqrt{\gamma}} + X \sqrt{\frac{2\gamma_b g}{\gamma^2}} \frac{\hat{B}_i^{in}}{\sqrt{\gamma}} \quad (i=3,4). \quad (23)$$

We finally end up with the four coupled equations

$$\begin{aligned} \frac{1}{\gamma} \frac{d}{dt} \hat{P}_1 = & \left[-1 - i \left(\Delta_1 + \frac{\hat{P}_1^\dagger \hat{P}_1}{2} + \hat{P}_2^\dagger \hat{P}_2 + \hat{Q}_1^\dagger \hat{Q}_1 + \hat{Q}_2^\dagger \hat{Q}_2 \right) \right] \hat{P}_1 \\ & - i \hat{P}_2^\dagger \hat{Q}_2 \hat{Q}_1 + \hat{P}_1^{in}, \end{aligned} \quad (24)$$

$$\begin{aligned} \frac{1}{\gamma} \frac{d}{dt} \hat{P}_2 = & \left[-1 - i \left(\Delta_2 + \hat{P}_1^\dagger \hat{P}_1 + \frac{\hat{P}_2^\dagger \hat{P}_2}{2} + \hat{Q}_1^\dagger \hat{Q}_1 + \hat{Q}_2^\dagger \hat{Q}_2 \right) \right] \hat{P}_2 \\ & - i \hat{P}_1^\dagger \hat{Q}_2 \hat{Q}_1 + \hat{P}_2^{in}, \end{aligned} \quad (25)$$

$$\begin{aligned} \frac{1}{\gamma} \frac{d}{dt} \hat{Q}_1 = & \left[-1 - i \left(\Delta_1 + \hat{P}_1^\dagger \hat{P}_1 + \hat{P}_2^\dagger \hat{P}_2 + \frac{\hat{Q}_1^\dagger \hat{Q}_1}{2} + \hat{Q}_2^\dagger \hat{Q}_2 \right) \right] \hat{Q}_1 \\ & - i \hat{Q}_2^\dagger \hat{P}_2 \hat{P}_1 + \hat{Q}_1^{in}, \end{aligned} \quad (26)$$

$$\begin{aligned} \frac{1}{\gamma} \frac{d}{dt} \hat{Q}_2 = & \left[-1 - i \left(\Delta_2 + \hat{P}_1^\dagger \hat{P}_1 + \hat{P}_2^\dagger \hat{P}_2 + \hat{Q}_1^\dagger \hat{Q}_1 + \frac{\hat{Q}_2^\dagger \hat{Q}_2}{2} \right) \right] \hat{Q}_2 \\ & - i \hat{Q}_1^\dagger \hat{P}_2 \hat{P}_1 + \hat{Q}_2^{in}, \end{aligned} \quad (27)$$

where the pump modes are noted as P while the modes generated by four-wave mixing are noted as Q .

III. STATIONARY SOLUTION

The steady state of the system [Eqs. (24)–(27)] is given by the solution of the following equations:

$$\begin{aligned} 0 = & \left[-1 - i \left(\Delta_1 + \frac{\bar{N}_{p_1}}{2} + \bar{N}_{p_2} + \bar{N}_{q_1} + \bar{N}_{q_2} \right) \right] \bar{P}_1 \\ & - i \bar{P}_2^* \bar{Q}_2 \bar{Q}_1 + \bar{P}_1^{in}, \end{aligned} \quad (28)$$

$$\begin{aligned} 0 = & \left[-1 - i \left(\Delta_2 + \bar{N}_{p_1} + \frac{\bar{N}_{p_2}}{2} + \bar{N}_{q_1} + \bar{N}_{q_2} \right) \right] \bar{P}_2 \\ & - i \bar{P}_1^* \bar{Q}_2 \bar{Q}_1 + \bar{P}_2^{in}, \end{aligned} \quad (29)$$

$$\begin{aligned} 0 = & \left[-1 - i \left(\Delta_3 + \bar{N}_{p_1} + \bar{N}_{p_2} + \frac{\bar{N}_{q_1}}{2} + \bar{N}_{q_2} \right) \right] \bar{Q}_1 - i \bar{Q}_2^* \bar{P}_2 \bar{P}_1, \end{aligned} \quad (30)$$

$$\begin{aligned} 0 = & \left[-1 - i \left(\Delta_4 + \bar{N}_{p_1} + \bar{N}_{p_2} + \bar{N}_{q_1} + \frac{\bar{N}_{q_2}}{2} \right) \right] \bar{Q}_2 - i \bar{Q}_1^* \bar{P}_2 \bar{P}_1. \end{aligned} \quad (31)$$

We set $\bar{N}_{p_1} = \bar{N}_{p_2} \equiv \bar{N}$ because the two pump beams intensities are equal. This allows us to cast Eq. (30) and the complex conjugate of Eq. (31) in the matrix form,

$$\mathbb{M} \begin{pmatrix} \bar{Q}_1 \\ \bar{Q}_2^* \end{pmatrix} = 0, \quad (32)$$

where \mathbb{M} is

$$\begin{pmatrix} -[1 + i(\Delta_3 + 2\bar{N})] & -i\bar{P}_1\bar{P}_2 \\ i\bar{P}_1^*\bar{P}_2^* & -[1 - i(\Delta_4 + 2\bar{N})] \end{pmatrix}. \quad (33)$$

Note that we neglect the population of the Q modes with respect to the pump modes, which is a valid approximation close to the oscillation threshold.

The oscillation condition $\bar{Q}_1, \bar{Q}_2 \neq 0$ imposes

$$\det \mathbb{M} = 0, \quad (34)$$

which gives

$$[1 + i(\Delta_3 + 2\bar{N})][1 - i(\Delta_4 + 2\bar{N})] - \bar{N}^2 = 0. \quad (35)$$

Straightforward algebra shows that $\Delta_3 = \Delta_4 \equiv \Delta$, i.e., the two generated modes necessarily have the same energy. The lowest threshold is obtained when the detuning compensates exactly the pump energy renormalization, that is, when $\Delta + 2\bar{N} = 0$. In this case the threshold condition becomes $\bar{N} = 1$. This value is identical to the one found in the theory of the polariton parametric oscillation.^{8,11} We stress that \bar{N} does not depend on the pump laser intensity. This is a well-known effect in triply resonant optical parametric oscillator (OPO) theory,²⁴ once the oscillation threshold has been reached, the intracavity intensity of the pump beam remains constant because all the energy injected by the pump is transferred to the signal and idler modes.

Our model allows to obtain an expression for the phases and intensities of the polariton fields, and their dependence on the pump field. The phases of the fields Q_1 and Q_2 can be obtained from the first line in Eq. (33), which reads

$$[1 + i(\Delta + 2\bar{N})]Q_1 = -i\bar{P}_1\bar{P}_2\bar{Q}_2^*. \quad (36)$$

Setting

$$\bar{Q}_i = |\bar{Q}_i|e^{i\varphi_i}, \quad (37)$$

$$\varphi_N = \arctan(\Delta + 2\bar{N}) \quad (38)$$

and choosing \bar{P}_1 and \bar{P}_2 reals we find the following relation for the phase sum:

$$\varphi_1 + \varphi_2 = -\varphi_N - \frac{\pi}{2}. \quad (39)$$

While the phase sum is fixed, the phase difference can change freely. This phase diffusion process is also typical of OPOs.²⁴

The intensities of the fields Q_1 and Q_2 are obtained from Eq. (36), which implies

$$|Q_1| = \frac{\bar{N}}{\sqrt{1 + (\Delta + 2\bar{N})^2}} |Q_2|. \quad (40)$$

Using Eq. (35), one can verify that

$$|\bar{Q}_1| = |\bar{Q}_2|. \quad (41)$$

The dependence on the pump-laser intensity can be derived by observing that, at threshold ($\bar{N} = 1$, $|\bar{Q}_1| = |\bar{Q}_2| = 0$), Eq. (28) can be expressed as

$$\left[1 + i\left(\Delta + \frac{3}{2}\right)\right]P_1 = \bar{P}_{1,s}^{in}, \quad (42)$$

where we have introduced the threshold value for the pump field $\bar{P}_{1,s}^{in}$. Above threshold, Eq. (28) becomes

$$i\bar{P}_2^*\bar{Q}_1\bar{Q}_2 = \bar{P}_1^{in} - \bar{P}_{1,s}^{in}. \quad (43)$$

Taking the square modulus, we obtain the dependence of the intensities of the modes Q_i on the pump rate σ ,

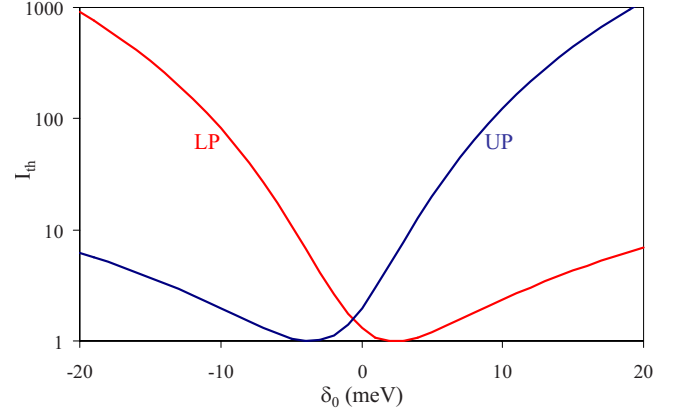


FIG. 3. (Color online) Threshold laser power for the upper and lower polariton branch, as a function of δ_0 , normalized to its minimum value.

$$|Q|^2 = |\bar{P}_{1,s}^{in}|(\sigma - 1) = \sqrt{1 + (\Delta + 3/2)^2}(\sigma - 1). \quad (44)$$

The parameter $\sigma = \sqrt{\frac{|\bar{P}_1^{in}|^2}{|\bar{P}_s^{in}|^2}} = \sqrt{\frac{\bar{P}_1^{in}}{\bar{P}_s^{in}}}$ represents the pump rate normalized to threshold. All our calculations are valid when $\sigma - 1 \ll 1$, which implies through Eq. (44) that $\bar{N}_{Q_i} \ll \bar{N}_{P_j}$.

We can now study the dependence of the oscillation threshold on the cavity-exciton detuning at normal incidence δ_0 . Equation (42), together with Eq. (22), allows us to write the expression for the laser power I_{th} (in units s^{-1}) required to reach the oscillation threshold,

$$I_{th} \approx \frac{\gamma^3}{2\gamma_a g C^2} = \frac{(C^2\gamma_a + X^2\gamma_b)^3}{2\gamma_a C^2(X^4V_0 + 4CX^3V_{sat})}. \quad (45)$$

We can introduce the weighted ratio of the photonic to the excitonic fraction s [Eq. (1)], to rewrite Eq. (45) as

$$I_{th} \approx \frac{\gamma_b^2}{2V_0} \frac{(1+s)^3}{s} \frac{1}{1 + 4\frac{V_{sat}}{V_0} \sqrt{\frac{\gamma_b}{\gamma_a}} \sqrt{s}}. \quad (46)$$

Expression (46) is valid also for the upper branch, with the substitutions (12) and (13). Experimentally, s can be controlled by changing the photonic and excitonic content of the pumped polaritons, which can be achieved by varying δ_0 .

I_{th} is plotted as a function of δ_0 in Fig. 3, for both polariton branches. The lowest threshold results from a trade-off between the excitonic fraction (required for efficient nonlinear interaction) and the photonic fraction (required for efficient coupling to the external cavity fields). The minimum value for laser power is obtained for $s \approx 1/2$.

IV. INTENSITY FLUCTUATIONS OF THE FIELDS

The aim of this section is to calculate the intensity fluctuations of the polariton fields and of the measurable extracavity photon fields. We recall that, for a generic field operator \hat{a} whose expectation value reads $|a|e^{-j\phi}$, the fluctuations δI of the associated intensity operator $I = \hat{a}^\dagger \hat{a}$ are proportional to the fluctuations of the amplitude quadrature $\alpha = \hat{a}e^{-j\phi} + \hat{a}^\dagger e^{+j\phi}$,

$$\delta I = |a|(\delta \hat{a} e^{-j\phi} + \delta \hat{a}^\dagger e^{+j\phi}). \quad (47)$$

In order to calculate the fluctuations of the field quadratures, we linearize Eqs. (24)–(27) around the following steady state:

$$\bar{P}_1 = \bar{P}_2 = \bar{P}_1^* = \bar{P}_2^* = 1, \quad (48)$$

$$\bar{Q}_1 = Q_0 \sqrt{\sigma - 1}, \quad (49)$$

$$\bar{Q}_2 = -i Q_0 \sqrt{\sigma - 1}, \quad (50)$$

where $Q_0 = \sqrt[4]{5/4}$.

This steady state is obtained when $\Delta = -2$ and $\bar{N} = 1$. Under such conditions, the laser detuning compensates the energy blueshift induced by the pump populations. The phase $\varphi_N = \arctan(\Delta + 2\bar{N})$ [Eq. (38)] is zero so that the phase between the conjugated fields is $-\pi/2$. This leads to a considerable simplification of the equations, allowing to find an analytical solution.

Operators \hat{P}_i are replaced by $\bar{P}_i + \delta \hat{P}_i$, and only the first-order terms are retained. We obtain the following equations for the signal and idler field fluctuations $\delta \hat{Q}_i$:

$$\begin{aligned} \frac{1}{\gamma} \frac{d}{dt} \delta \hat{Q}_1 &= Q_0 \sqrt{\sigma - 1} (1 - i) (\delta \hat{P}_1 + \delta \hat{P}_2) \\ &\quad - i Q_0 \sqrt{\sigma - 1} (\delta \hat{P}_1^\dagger + \delta \hat{P}_2^\dagger) - \delta \hat{Q}_1 - i \delta \hat{Q}_2^\dagger + \delta Q_1^{in}, \end{aligned} \quad (51)$$

$$\begin{aligned} \frac{1}{\gamma} \frac{d}{dt} \delta \hat{Q}_2 &= Q_0 \sqrt{\sigma - 1} (-1 - i) (\delta \hat{P}_1 + \delta \hat{P}_2) \\ &\quad - Q_0 \sqrt{\sigma - 1} (\delta \hat{P}_1^\dagger + \delta \hat{P}_2^\dagger) - \delta \hat{Q}_2 - i \delta \hat{Q}_1^\dagger + \delta Q_2^{in}. \end{aligned} \quad (52)$$

We introduce the Hermitian operators

$$\hat{\alpha}_{Q_1} = \delta \hat{Q}_1 + \delta \hat{Q}_1^\dagger, \quad (53)$$

$$\hat{\beta}_{Q_2} = i(\delta \hat{Q}_2^\dagger - \delta \hat{Q}_2) \quad (54)$$

representing the amplitude fluctuations of the modes Q_i . These operators evolve according to

$$\frac{1}{\gamma} \frac{d}{dt} \hat{\alpha}_{Q_1} = Q_0 \sqrt{\sigma - 1} (\hat{\alpha}_{P_1} + \hat{\alpha}_{P_2}) - \hat{\alpha}_{Q_1} + \hat{\beta}_{Q_2} + \hat{\alpha}_{Q_1}^{in}, \quad (55)$$

$$\frac{1}{\gamma} \frac{d}{dt} \hat{\beta}_{Q_2} = Q_0 \sqrt{\sigma - 1} (\hat{\alpha}_{P_1} + \hat{\alpha}_{P_2}) - \hat{\beta}_{Q_2} + \hat{\alpha}_{Q_1} + \hat{\beta}_{Q_2}^{in}. \quad (56)$$

We are now in position to calculate the difference of the amplitude fluctuations $\hat{r}' = \frac{1}{2}(\hat{\alpha}_{Q_1} - \hat{\beta}_{Q_2})$,

$$\frac{1}{\gamma} \frac{d}{dt} \hat{r}' = -2\hat{r}' + \hat{r}'^{in}. \quad (57)$$

As in OPOs, \hat{r}' is independent of the pump fields fluctuations. The nonclassical effects in OPOs benefit from this property. Equation (57) shows that it also arises in polariton four-wave mixing.

An equation identical to Eq. (57) holds for the operator $\hat{r} = \frac{1}{\sqrt{2}}(\hat{\alpha}_{P_3} - \hat{\beta}_{P_4})$ describing the difference of amplitude fluctuations of the polariton operators \hat{p}_3 and \hat{p}_4 ,

$$\frac{d}{dt} \hat{r} = -2\gamma \hat{r} + \hat{r}^{in}. \quad (58)$$

The input noise operator \hat{r}^{in} in Eq. (58) reads

$$\hat{r}^{in} = \frac{1}{\sqrt{2}}(\hat{\alpha}_{P_3}^{in} - \hat{\beta}_{P_4}^{in}) = -C\sqrt{2\gamma_a} \hat{r}_A^{in} + X\sqrt{2\gamma_b} \hat{r}_B^{in}, \quad (59)$$

where $\hat{r}_A^{in} = \frac{1}{\sqrt{2}}(\hat{\alpha}_{A_3}^{in} - \hat{\beta}_{A_4}^{in})$ and $\hat{r}_B^{in} = \frac{1}{\sqrt{2}}(\hat{\alpha}_{B_3}^{in} - \hat{\beta}_{B_4}^{in})$.

In Eq. (59), the excitonic and photonic input noises appear again explicitly. By Fourier transforming, one obtains

$$\hat{r}(\Omega) = \frac{1}{2\gamma - i\Omega} \hat{r}^{in}(\Omega). \quad (60)$$

This result allows us to calculate the extracavity photonic field fluctuations. The extracavity field is related to the intracavity and input field by the input-output relation

$$\hat{a}^{out} = \sqrt{2\gamma_a} \hat{a} - \hat{a}^{in}. \quad (61)$$

Given the energy separation between upper and lower polariton branches, the intracavity electromagnetic field can be taken as simply proportional to the polariton field,¹¹

$$\hat{a}^{out} = -C\sqrt{2\gamma_a} \hat{p} - \hat{a}^{in}. \quad (62)$$

The operator \hat{r}_A^{out} describing the difference of the amplitude fluctuations of the extracavity fields reads

$$\hat{r}_A^{out} = -C\sqrt{2\gamma_a} \hat{r} - \hat{r}_A^{in}. \quad (63)$$

Inserting Eqs. (59) and (60) in Eq. (63), one obtains

$$\hat{r}_A^{out} = \left(\frac{2\gamma_a C^2}{2\gamma - i\Omega} - 1 \right) \hat{r}_A^{in} - \frac{2XC\sqrt{\gamma_a \gamma_b}}{2\gamma - i\Omega} \hat{r}_B^{in}. \quad (64)$$

The noise spectrum of the extracavity intensity difference fluctuations $S_r^{out} = \langle \hat{r}_A^{out}(\Omega) \hat{r}_A^{out}(-\Omega) \rangle$ of \hat{r}_A^{out} , normalized to the standard quantum limit (SQL), reads

$$\begin{aligned} S_r^{out} &= 1 + \frac{4\gamma_a \gamma_b C^2 X^2}{4\gamma^2 + \Omega^2} [\langle \hat{r}_B^{in}(\Omega) \hat{r}_B^{in}(-\Omega) \rangle - 1] \\ &\quad - 4 \frac{\gamma_a C^2 \gamma}{4\gamma^2 + \Omega^2} \langle \hat{r}_A^{in}(\Omega) \hat{r}_A^{in}(-\Omega) \rangle. \end{aligned} \quad (65)$$

The experimentally accessible frequencies are much lower than γ , therefore we essentially measure noise at zero frequency. The input noise for the electromagnetic field $\langle \hat{r}_A^{in}(\Omega) \hat{r}_A^{in}(-\Omega) \rangle$ can be assumed to be equal to 1 at all frequencies, i.e., the input photon field for the modes q_i is a vacuum state. Using these two facts Eq. (65) can be put in a

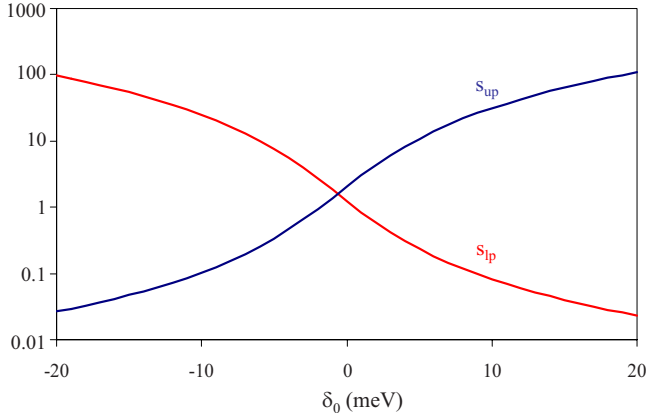


FIG. 4. (Color online) Weighted ratio of the photonic to the excitonic fraction s [Eq. (1)] as a function of δ_0 for the upper and lower polariton branch.

form where only the weighted ratio of the photonic to the excitonic fraction s [Eq. (1)] appears

$$S_r^{out} = 1 + \frac{s}{(1+s)^2} E - \frac{s}{1+s}, \quad (66)$$

where $E = [\langle \hat{r}_B^{in}(\Omega) \hat{r}_B^{in}(-\Omega) \rangle - 1]$ is the input excess noise coming from the exciton reservoir.

V. DISCUSSION

As anticipated, the squeezing properties of the output field depend only on s and on the input excess noise E coming from the exciton reservoir. s is plotted as a function of δ_0 for the two branches in Fig. 4. For the lower polariton branch s increases for negative detunings because in this case the lower-branch polaritons have an important photonic content. For the same reason, s increases for positive detunings for the upper-branch polaritons.

The noise spectrum of the extracavity intensity difference fluctuations S_r^{out} is plotted in Figs. 5 and 6. It is compared to the SQL, which is normalized to 1 in our equations. The

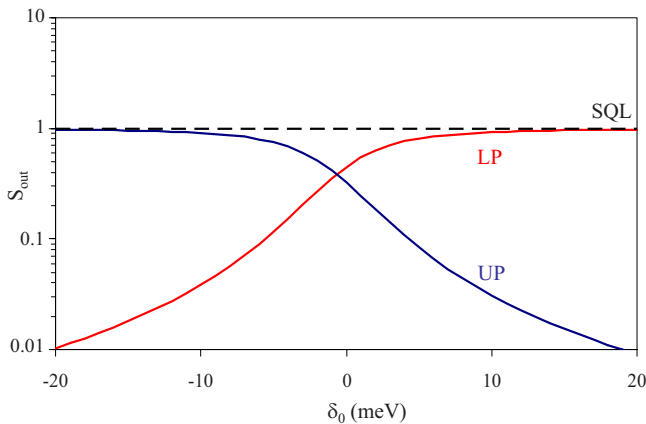


FIG. 5. (Color online) Noise of the intensity difference of the extracavity photon fields as a function of δ_0 for the upper and lower polariton branch. Ideal case: excitonic input excess noise $E=0$.

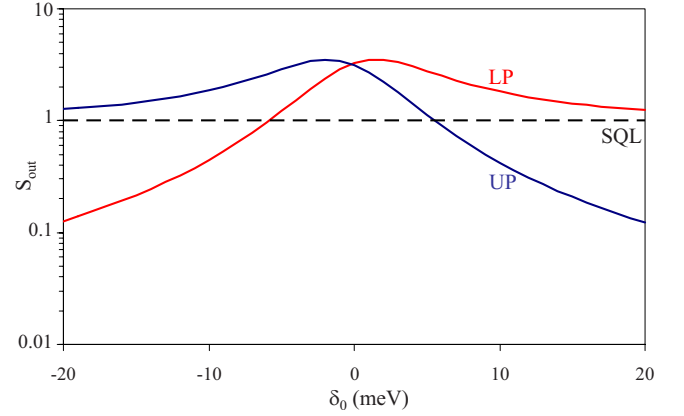


FIG. 6. (Color online) Noise of the intensity difference of the extracavity photon fields as a function of δ_0 for the upper and lower polariton branch. Excitonic input excess noise $E=12$, corresponding to the experimental data reported in Ref. 22.

SQL is the noise that would be obtained if, for instance, one splits a laser beam in two parts of the same power using a linear beam splitter, and then subtracts their intensity fluctuations. This thought experiment shows that one cannot obtain by a linear optical process two perfect copies of the same state of radiation; the quantum fluctuations of the two beams are perfectly uncorrelated. In order to go below the SQL, one has to introduce quantum correlations between the two beams using some optical nonlinearities. For instance, in our case polaritons are produced in pairs by the four-wave mixing process; the creation of one polariton in the signal mode implies necessarily the creation of one polariton in the idler, therefore ideally we expect that the intensity fluctuations are exactly the same in the two modes, which means squeezing of the intensity difference fluctuations.

If there is no input excess noise, the model predicts squeezing for all values of δ_0 for both branches (see Fig. 5). The squeezing vanishes as the polariton becomes more and more excitonlike while it increases and tends to become perfect as the polariton becomes more and more photonlike.

In presence of excitonic excess noise E , Eq. (66) states that s must satisfy the following inequality in order to have squeezing:

$$s > E - 1. \quad (67)$$

The inequality in Eq. (67) can always be satisfied for some value of δ_0 . Physically this means that, if an important amount of noise enters from the excitonic port, a polariton mode with a sufficiently large photonic fraction must be chosen in order to efficiently filter out the excitonic noise. We stress that, in this respect, the four-wave mixing scheme demonstrated in Ref. 15 is particularly adapted because energy conservation is automatically fulfilled for any value of δ_0 or any angle of incidence. The nonlinear process is perfectly independent of the polariton dispersion and therefore the photonic and excitonic content of the polaritons can be tuned freely.

One may ask if the input excitonic noise E changes with δ_0 . In order to examine this point, we need to recall the

physical origin of the excess noise. As discussed in Refs. 18 and 25, besides polariton-polariton scattering, the relaxation of polaritons is due to polariton-phonon scattering, which is then responsible, through the fluctuation-dissipation theorem, of the input excess noise. The phonon-polariton scattering rate is roughly proportional to the density of states of the polariton modes at the scattering energy.²⁵ Now, as δ_0 decreases, as it is needed in order to obtain squeezing, the slope of the polariton energy dispersion becomes steeper and steeper [as can be verified calculating $\frac{\partial E_{LP}}{\partial k}$ from Eq. (9)]. This can be easily understood because polaritons become more and more photonlike. Now, a steeper dispersion implies that fewer final states are available in the energy range than can be reached by phonon scattering; the overall polariton-phonon scattering rate should then diminish. In conclusion, when δ_0 is decreased there is another mechanism that reduces the coupling to phonons, besides the filtering effect obtained by reducing the excitonic fraction of the polariton. This mechanism should reduce the value of E when δ_0 is decreased. So, considering E as constant is actually a simplifying hypothesis that looks quite conservative; the values of δ_0 obtained from Eq. (67) can be viewed as upper bounds for the appearance of quantum effects.

In practice, the major drawback will probably come from the fact that the oscillation threshold increases rapidly with s , as shown in Fig. 3. The experimental data available allow to give the following estimations. In Ref. 15, the incidence angle was of 6° . Assuming a resonant excitation of the lower polariton, this corresponds to $s_{exp}=1.24$. S_r^{out} was roughly equal to 10. Equation (66) permits to estimate $E=40$. From Eq. (67), we obtain $s_{sq}=39$ as the lowest value for s in order to have squeezing. Using Eq. (46) we see that I_{th} will be increased by a factor of about 130. The threshold for four-wave mixing oscillation was 15 mW. In order to observe squeezing, the microcavity should be resonantly pumped at a negative detuning $\delta_0 \simeq -13$ meV for the lower branch, with 2 W of power for each pump beam.

Data from Ref. 22 report observation of polariton four-wave mixing oscillation at $i=3^\circ$, with a threshold power of 7.5 mW, with a positive cavity-exciton detuning of 1.1 meV. S_r^{out} was measured to be 3.5. In this case, we find that pumping the lower branch at a negative detuning of -6.3 meV would allow to see quantum effects (see Fig. 6). In this case the threshold is expected to increase in a factor of about 20, corresponding to 150 mW for each pump beam, which corresponds to a more favorable case than the previous one and allows to predict squeezing for experimentally feasible parameters. In order to have a noise reduction of 3 dB below the standard quantum limit, one should resonantly pump at a negative detuning of -9 meV; in such conditions, four-wave mixing oscillation would appear for a pump power of 450 mW for each pump beam.

VI. CONCLUSIONS

In conclusion, we have provided an analytical model describing polariton four-wave mixing oscillation, slightly above the oscillation threshold. Linearized expressions for the intensity noise spectra of the extracavity photon fields have been derived. It has been shown that the squeezing properties of the generated fields depend essentially on the weighted ratio of the photonic to the excitonic fraction of the generated modes. From our analysis it results that photonlike polaritons are more adapted for the generation of squeezed field states, mainly because they permit to filter out the excitonic noise contribution. Four-wave mixing oscillation requires higher pump power for photonlike polaritons, but an estimation based on available experimental data indicates that it should be within reach experimentally.

ACKNOWLEDGMENTS

Some of us (E.G. and A.B.) acknowledge support from the ANR contract ‘‘GEMINI’’ (Grant No. ANR-07-NANO-005) and from the FP7 ITN ‘‘Clermont4’’ (235114).

¹J. Kasprzak, M. Richard, S. Kundermann, A. Baas, P. Jeambrun, J. M. J. Keeling, F. M. Marchetti, M. H. Szymańska, R. André, J. L. Staehli, V. Savona, P. B. Littlewood, B. Deveaud, and L. Si Dang, *Nature (London)* **443**, 409 (2006).

²S. Utsunomiya, L. Tian, G. Roumpos, C. W. Lai, N. Kumada, T. Fujisawa, M. Kuwata-Gonokami, A. Löffler, S. Höfling, A. Forchel, and Y. Yamamoto, *Nat. Phys.* **4**, 700 (2008).

³A. Amo, D. Sanvitto, F. P. Laussy, D. Ballarini, E. del Valle, M. D. Martin, A. Lemaître, J. Bloch, D. N. Krizhanovskii, M. S. Skolnick, C. Tejedor, and L. Viña, *Nature (London)* **457**, 291 (2009).

⁴A. Amo, J. Lefrère, S. Pigeon, C. Adrados, C. Ciuti, I. Carusotto, R. Houdré, E. Giacobino, and A. Bramati, *Nat. Phys.* **5**, 805 (2009).

⁵P. G. Savvidis, J. J. Baumberg, R. M. Stevenson, M. S. Skolnick, D. M. Whittaker, and J. S. Roberts, *Phys. Rev. Lett.* **84**, 1547 (2000).

⁶G. Messin, J. P. Karr, A. Baas, G. Khitrova, R. Houdré, R. P. Stanley, U. Oesterle, and E. Giacobino, *Phys. Rev. Lett.* **87**, 127403 (2001).

⁷M. Saba, C. Ciuti, J. Bloch, V. Thierry-Mieg, R. André, L. Si Dang, S. Kundermann, A. Mura, G. Bongiovanni, J. L. Staehli, and B. Deveaud, *Nature (London)* **414**, 731 (2001).

⁸C. Ciuti, P. Schwendimann, and A. Quattropani, *Semicond. Sci. Technol.* **18**, S279 (2003).

⁹G. Messin, J. Ph. Karr, H. Eleuch, J. M. Courty, and E. Giacobino, *J. Phys.: Condens. Matter* **11**, 6069 (1999).

¹⁰P. Schwendimann, C. Ciuti, and A. Quattropani, *Phys. Rev. B* **68**, 165324 (2003).

¹¹J.-Ph. Karr, A. Baas, and E. Giacobino, *Phys. Rev. A* **69**, 063807 (2004).

¹²C. Ciuti, *Phys. Rev. B* **69**, 245304 (2004).

¹³J.-Ph. Karr, A. Baas, R. Houdré, and E. Giacobino, *Phys. Rev. A* **69**, 031802(R) (2004).

- ¹⁴S. Savasta, O. Di Stefano, V. Savona, and W. Langbein, *Phys. Rev. Lett.* **94**, 246401 (2005).
- ¹⁵M. Romanelli, C. Leyder, J. Ph. Karr, E. Giacobino, and A. Bramati, *Phys. Rev. Lett.* **98**, 106401 (2007).
- ¹⁶A. Verger, I. Carusotto, and C. Ciuti, *Phys. Rev. B* **76**, 115324 (2007).
- ¹⁷S. Portolan, O. Di Stefano, S. Savasta, F. Rossi, and R. Girlanda, *Phys. Rev. B* **77**, 195305 (2008).
- ¹⁸S. Portolan, O. Di Stefano, S. Savasta, F. Rossi, and R. Girlanda, *Phys. Rev. B* **77**, 035433 (2008).
- ¹⁹S. Portolan, O. Di Stefano, S. Savasta, and V. Savona, *EPL* **88**, 20003 (2009).
- ²⁰R. Houdré, C. Weisbuch, R. P. Stanley, U. Oesterle, and M. Illegems, *Phys. Rev. B* **61**, R13333 (2000).
- ²¹I. A. Shelykh, A. V. Kavokin, and G. Malpuech, *Phys. Status Solidi B* **242**, 2271 (2005).
- ²²C. Leyder, *Optique quantique et dynamique de spin dans les microcavités semi-conductrices*, Ph.D. thesis, 2007. <http://tel.archives-ouvertes.fr/tel-00169855/fr>.
- ²³F. Tassone and Y. Yamamoto, *Phys. Rev. B* **59**, 10830 (1999).
- ²⁴C. Fabre, E. Giacobino, A. Heidmann, and S. Reynaud, *J. Phys. (France)* **50**, 1209 (1989).
- ²⁵F. Tassone, C. Piermarocchi, V. Savona, A. Quattropani, and P. Schwendimann, *Phys. Rev. B* **56**, 7554 (1997).